Volume 240, number 1,2, 88–94 FEB 06514 November 1988

Intracellular calcium release mediated by two muscarinic receptor subtypes

Erwin Neher, Alain Marty+, Kazuhiko Fukuda°, Tai Kubo° and Shosaku Numa°

Max-Planck-Institut für biophysikalische Chemie, D-3400 Göttingen, FRG, +Laboratoire de Neurobiologie, Ecole Normale Superieure, F-75230 Paris Cédex 05, France and *°Departments of Medical Chemistry and Molecular Genetics, Kyoto University, Faculty of Medicine, Kyoto 606, Japan*

Received 4 October 1988

Four subtypes of muscarinic acetylcholine receptor (mAChR) were stably expressed in neuroblastoma-glioma hybrid cells (NG108-15). By combining fluorescent indicator dye (fura-2) studies with electrophysiological measurements it is shown that stimulation of mAChR I and mAChR III readily leads to release of calcium from intracellular stores and to associated conductance changes, whereas stimulation of mAChR II and mAChR IV exerts no such effect. Dose-response curves describing the amplitude or the delay of the calcium rise induced by acetylcholine suggest that the apparent affinity of mAChR III for its agonist is higher by about one order of magnitude than that of mAChR I. Ionic substitution experiments and current fluctuation analysis indicate that calcium activates a K^+-specific conductance of 'small' single-channel amplitude similar to the SK type [1]. Furthermore, an outward current (M current) suppressed by activation of mAChR I and mAChR III has a single-channel amplitude corresponding to a conductance of approximately 3 pS.

Muscarinic acetylcholine receptor subtype; Ca^{2+} release; Ca^{2+}-activated current; M current; (Neuroblastoma-glioma hybrid cell)

1. INTRODUCTION

Muscarinic cholinergic receptors mediate a variety of cellular responses including increases in the concentration of free intracellular calcium ($[Ca^{2+}]_i$) and induction of Ca^{2+}-dependent currents [2], modulation of Ca^{2+} currents [3], activation of K^+ currents [4,5], and suppression of M currents [6]. Expression of cloned cDNAs or genomic DNAs encoding four different subtypes of mAChR [7–18] has made it possible to assign some of the diverse effects to specific subtypes. Thus, expression studies with *Xenopus* oocytes have provided evidence that mAChR I, unlike mAChR II, principally mediates Ca^{2+}-induced currents [8]. Furthermore, stable expression of four subtypes in different mammalian cell lines has led to the conclusion that mAChR I and mAChR III are coupled with stimulation of PI hydrolysis [9,15,18], whereas mAChR II and mAChR IV are linked mainly with inhibition of adenylate cyclase [14,15]. Note that mAChR III and mAChR IV are defined as in [16] and correspond to HM4 and HM3 in [13], respectively. mAChR I and mAChR III expressed in mammalian cells, as well as in *Xenopus* oocytes, elicit current responses to muscarinic stimulation which are indicative of $[Ca^{2+}]_i$ elevation following PI breakdown [8,9,11,17]. Furthermore, mAChR I and mAChR III mediate inhibition of the M current in stably transformed neuroblastoma-glioma hybrid cells (NG108-15) [9]. The main purpose of the present investigation is to directly demonstrate increases in $[Ca^{2+}]_i$ in transformed NG108-15 cells using the fluorescent indicator dye fura-2 and to describe their temporal characteristics dependent on agonist concentration in cells expressing different mAChR

Correspondence address: E. Neher, Max-Planck-Institut für biophysikalische Chemie, Postfach 2841, D-3400 Göttingen, FRG

Abbreviations: mAChR, muscarinic acetylcholine receptor; ACh, acetylcholine; QNB, quinuclidinyl benzilate; PI, phosphoinositides

Published by Elsevier Science Publishers B.V. (Biomedical Division)
00145793/88/$3.50

subtypes. Concomitant changes in membrane conductance are also analyzed.

2. MATERIALS AND METHODS

NG108-15 cells [19,20] were transfected with cDNA or genomic DNA encoding each of the four mAChR subtypes as described in [9]. The clones described in [9] were used to screen for $[Ca^{2+}]_i$ changes. In addition the porcine mAChR I-transformed clone NGPM1-30 (transfected with the plasmid pKPM1 [9]) was used. All the clones used had (−)-[^{3}H]quinuclidinyl benzilate (QNB) binding activities (determined as in [9]) at least three times the value of nontransfected cells. Cells were cultured in DMEM (Gibco) supplemented with 10% fetal calf serum, 50 μg/ml streptomycin, 50 units/ml penicillin, 1 mM Na-pyruvate, 100 μM hypoxanthine, 1 μM aminopterin and 16 μM thymidine. One day to one week prior to the experiment cells were plated onto coverslips, which were later on transferred to the experimental chamber.

Patch-clamp measurements were performed in a saline of the following composition (in mM): 145 NaCl; 5.5 KCl; 1 $MgCl_2$; 2 $CaCl_2$; 10 Hepes-NaOH; pH 7.2, unless specified otherwise. Patch pipettes were filled with a solution of the following composition (in mM): 145 K-glutamate; 8 NaCl; 1 $MgCl_2$; 10 Hepes-KOH; 0.5 MgATP; 0.3 GTP; 0.1 fura-2 pentapotassium salt (Molecular Probes); pH 7.2. Patch pipettes ranged in resistance from 2 to 5 MΩ. Membrane potential was clamped to values between −40 mV and −80 mV and depolarizing and hyperpolarizing voltage-clamp commands were applied in the tight-seal whole cell configuration [21]. Simultaneously $[Ca^{2+}]_i$ was measured by the fura-2 method [22] as described in [23,24]. Cells of approx. 20–30 μm diameter with 15–30 pF capacitance were selected. Both differentiated and nondifferentiated cells were used. The bulk of measurements was performed on nondifferentiated cells since both types showed similar Ca^{2+} transients.

For fura-2-ester loading, cells were incubated for 30 min in 1–5 μM fura-2-AM (Molecular Probes) in normal saline at room temperature. The fura-2-ester concentration had to be adjusted in this range depending on the density of cells, 2 ml of the highest concentration being sufficient for an almost complete monolayer of cells on a round, 10 mm diameter coverslip. Thereafter cells were washed twice and incubated in saline at 37°C for 15 min. Measurements were made within 60 min following the ester loading procedure. Autofluorescence of 5 to 10 cells was repeatedly measured in dishes of cells that had not been ester-loaded. The average of this background was subtracted from the fluorescence values of ester-loaded cells. It typically was 5–10% of the final signal. Acetylcholine (ACh) was applied locally from a puffer pipette of 2–3 μm diameter for 4–25 s and the dish was rinsed with ACh-free solution within another 5 s. Alternatively the dish was continuously perfused (1 exchange per min) for removal of the ACh. Up to 15 cells were tested in one dish. Care was taken to use cells that were at least 0.5–1 mm apart. Otherwise cells might have been desensitized by previous ACh applications. The pressure in the puffer pipette was electronically controlled. This allowed a precise timing of the ACh application. In control experiments for testing the application procedure, fluorescent dye was filled into the pipette. These tests showed that the entire volume, which during a recording would contain the cell, was uniformly flooded by the test solution within 1 s. The final fluorescence measured was equal to that measured during bath perfusion of the same solution, indicating that no dilution occurred.

All experiments were performed at room temperature (22–25°C). Average values are given as mean ± SE (number of experiments).

3. RESULTS

3.1. *Measurements of $[Ca^{2+}]_i$ in fura-2-ester-loaded cells*

Neuroblastoma-glioma hybrid cells (NG108-15), loaded with the membrane-permeable ester fura-2-AM, were stimulated with ACh at concentrations ranging from 0.02 to 50 μM. In control cells (nontransfected and vector-transformed), this led to changes in $[Ca^{2+}]_i$ only in exceptional cases (four slow and very small responses in 32 cells studied). Also, in nontransfected cells from another source (108CC15 cells [20] kindly provided by Drs B. Hamprecht and G. Reiser, University of Tübingen) 50 μM ACh elicited responses in less than 10% of cases. In NG108-15 cells transformed to express mAChR II or mAChR IV, the fraction of cells that responded to ACh concentrations of 5–50 μM was comparable (< 10%) to that of control cells.

In contrast, NG108-15 cells transformed to express either mAChR I or mAChR III consistently showed transient increases in $[Ca^{2+}]_i$ following stimulation with ACh. Fig.1A shows the range of responses at saturating ACh concentration (5 μM) in the case of mAChR I-transformed cells. $[Ca^{2+}]_i$, typically after a short delay, rose from a basal value of 0.1–0.3 μM to values between 1 and 3 μM and then gradually declined in 10–20 s back to near-basal values. The decline was observed both when the stimulation was continuous and when it was discontinued after 5–10 s. When short stimuli of 1–2 s duration were applied, some cells responded after the end of the stimulus. Fig.1B shows responses at a low concentration of ACh (0.4 μM). Here responses on average were smaller (note different scale) and had a longer delay and a somewhat slower decay. However, also at this low concentration there was usually a pronounced decline in $[Ca^{2+}]_i$ before the end of the stimulus. At still lower concentrations of ACh an increasing fraction of cells failed to respond at all.

Fig.1C shows mean amplitudes as a function of

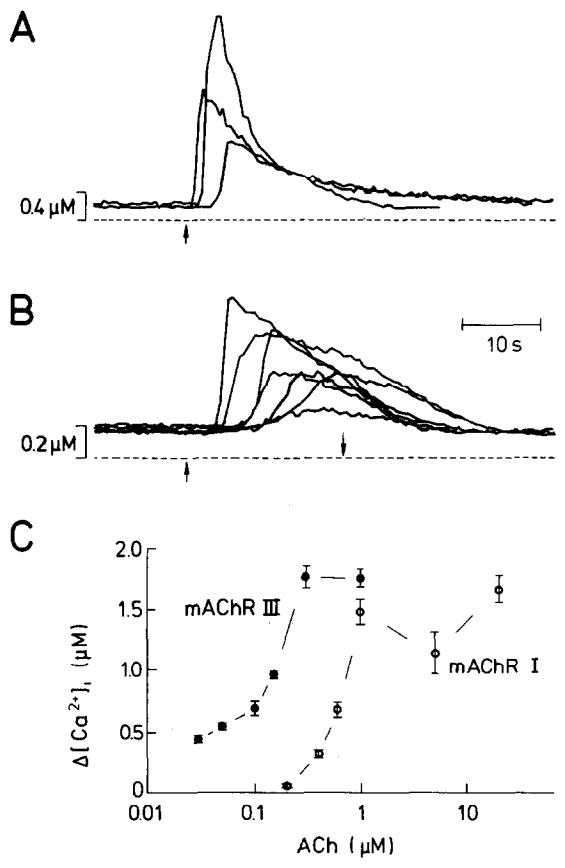

Fig.1. Representative superimposed examples of calcium signals at a saturating ACh concentration of 5 μM (A) and at 0.4 μM (B). Clone NGPM1-27 (porcine mAChR I-transformed) was used. The onset of ACh applications is marked by an upward arrow in both A and B; the end of applications is indicated by the downward arrow in B. In A, ACh application varied in length between 12 and 25 s. The baselines are marked by broken lines. (C) Plot of mean increment in $[Ca^{2+}]_i$ versus ACh concentration for transformed cells with porcine mAChR I (○, clone NGPM1-27) or porcine mAChR III (●, clone NGPM3-332). Each symbol represents a mean of 7–25 measurements, which also includes zeroes (response failures). These had negligible influence in the case of mAChR III data, however they reduced values for mAChR I by 10–40%. Error bars indicate SE.

ACh concentration, comparing two clones expressing mAChR I and mAChR III, respectively. These dose-response curves give similar maximum responses for the two clones, but they show an almost 10-fold higher sensitivity to ACh for mAChR III-transformed cells as compared with mAChR I-transformed cells. The same concentration shift was also observed with respect to the kinetics of the responses. At ACh concentrations that gave full amplitude responses, $[Ca^{2+}]_i$ typically rose sharply following short delays of 1–4 s, while at lower ACh concentrations the rise was slower, starting only after delays of 4–15 s. Responses with delays longer than 15 s were rarely observed. These observations were made for both mAChR I-transformed and mAChR III-transformed cells. Thus, the mechanism for Ca^{2+}-release seems to be similar for mAChR I and mAChR III, except for a higher ACh sensitivity of mAChR III.

A quantitative analysis of the delay as a function of ACh concentration was carried out to examine further the difference between mAChR I-transformed and mAChR III-transformed cells. The rationale of this analysis derives from a theory of muscarinic action which relates delay to receptor activation [25]. This theory predicts that a plot of the delay as a function of the reciprocal of ACh concentration should give a straight line, the negative x-intercept providing an estimate for the apparent dissociation constant K_D. Fig.2 compares such a plot for an mAChR I-transformed clone with that of an mAChR III-transformed clone. Absolute values of delays vary between batches of cells within about a factor of two. Therefore plots like those shown in fig.2 were obtained from cells out of one culture dish each. Apparent K_D values derived from these plots were always very different between mAChR I-transformed and mAChR III-transformed cells. Table 1 presents parameters for four different clones.

The responses described above did not depend on the presence of extracellular Ca^{2+}. When cells (porcine mAChR I-transformed clone NGPM1-27) were incubated for 1–10 min in Ca^{2+}-free saline (3 cells) or in Ca^{2+}-free saline supplemented with 1 mM EDTA (10 cells), responses to stimulation with 20 μM ACh were not noticeably different from those of untreated cells.

3.2. *Measurements on cells under patch clamp*

mAChR I-transformed and mAChR III-transformed cells as well as nontransfected cells were studied under patch-clamp conditions in the tight seal whole-cell recording mode. In these experiments they were not pretreated with fura-2 ester, but the free salt was loaded into the cells through the recording pipette [23,24]. Ca^{2+} tran-

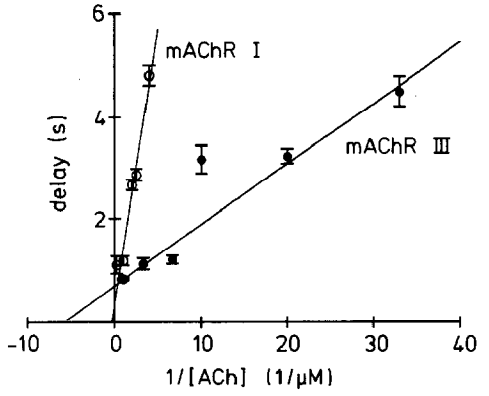

Fig.2. Mean latency of the response plotted against the reciprocal of ACh concentration for porcine mAChR I-transformed cells (○, clone NGPM1-27) compared with porcine mAChR III-transformed cells (●, clone NGPM3-332). Mean latency is defined as the time between onset of the stimulus (after correcting for the system dead time) and half-maximal response. Each data point represents the mean of responses from 10 to 20 cells. Within each plot, data were obtained from cells of the same batch. Failures were disregarded, but analysis was restricted to runs with less than 20% failures. Straight lines represent least-square fits with data weighted according to SE as indicated by the bars.

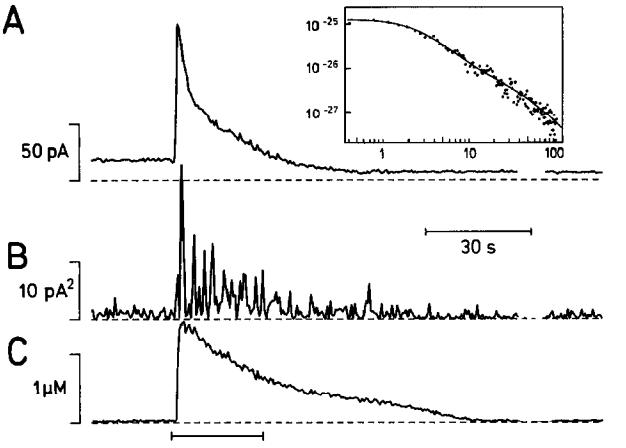

Fig.3. Calcium and current signals under whole-cell patch-clamp conditions following application of 20 μM ACh (bar) to a porcine mAChR I-transformed cell (clone NGPM1-27). (A) Holding current at −40 mV potential. (B) Current variance calculated on 0.5 s current segments after low pass filtering at 500 Hz (4-pole Butterworth filter). (C) $[Ca^{2+}]_i$. The baselines are indicated by broken lines. Recording was interrupted for 8 s during the gap towards the end of the record. The inset shows a double logarithmic plot of noise power spectral density with a two-component Lorentzian fit in the frequency range from 0.4 to 100 Hz. The units given on the y-axis are A^2/Hz; the x-axis is calibrated in Hz. The fitted parameters are: zero frequency asymptotes $A_1 = 1.2 \times 10^{-25}$ A^2/Hz; $A_2 = 0.5 \times 10^{-26}$ A^2/Hz; corner frequencies $F_1 = 2.8$ Hz; $F_2 = 35$ Hz. The spectrum represents the difference between two runs before and after ACh application, respectively. DC currents differ by 10.3 pA for the two runs. The ratio of the integral of the double Lorentzian curve over the difference in mean current yields a single-channel amplitude of 0.08 pA.

sients very similar to those described above were observed, as exemplified in fig.3C. The mean increment of $[Ca^{2+}]_i$ of responding cells under these conditions (pooled data from clones NGPM1-3, NGPM1-27 and NGPM3-332 at 2–20 μM ACh) was 1.05 ± 0.14 μM (n = 38).

The cell presented in fig.3 was held at −40 mV. Before application of ACh (20 μM) a holding current of +18 pA was required. Concomitantly with the Ca^{2+} transient, the holding current went through a peak of approx. 150 pA and then declined to a level lower than before (fig.3A). This finding is very similar to that of Fukuda et al. [9], who have concluded that the current response results from activation of a Ca^{2+}-induced K^+ current followed by suppression of the M current. As in [9], we found that the late current decrease was accompanied by a reduction in the amplitude of slow voltage-induced relaxations characteristic of M currents. However, the M current decrease was irreversible under our recording conditions even though that obtained in microelectrode experiments reverts by a few minutes' wash [9]. We characterized the currents further by analyzing current fluctuations associated with them. Fig.3B represents variance of the current as determined in

Table 1

Dissociation constants (K_D') and limiting delay times (t_∞) derived from latency plots

mAChR subtype	Clone	(−)-[^{3}H]QNB binding (fmol per mg protein)	K_D' (μM)	t_∞ (s)
Porcine mAChR I	NGPM1-27[a]	1182[b]	3.0	0.4
	NGPM1-27[a]		3.0	0.9
	NGPM1-30	939	1.7	0.7
Porcine mAChR III	NGPM3-332	842[b]	0.17	0.7
	NGPM3-161	424[b]	0.23	1.3

[a] Two different batches of cells
[b] Taken from [9]

0.5 s segments with a bandwidth of 500 Hz. It is seen that the variance goes through a pronounced peak as long as the Ca^{2+}-induced current is high. When the variance increment is divided by the current increment (both with respect to the previous baseline), an estimate for the Ca^{2+}-induced single-channel current of 0.094 pA is obtained, assuming small open probability of the channel. This, together with a reversal potential of the Ca^{2+}-induced current of −72 mV (see below), gives a single-channel conductance of 2.9 pS. The mean single-channel conductance was 2.72 ± 0.3 pS (n = 5).

As the outward current subsided, the variance decreased below the value obtained before ACh application. This could be identified on the oscilloscope as a reduction of slow current fluctuations. Noise spectral analysis [26] yielded spectra which could be well fitted by two Lorentzian components (fig.3A, inset) with corner frequencies at 2 Hz and 35–40 Hz, respectively. The single-channel conductance estimate for the M current obtained as the ratio of the difference of variance over that of the mean current was 3.15 ± 0.7 pS (n = 4). It should be noted that the numbers obtained for the Ca^{2+}-dependent K^+ channel and for the M channel assume low probability of channel opening and also reflect the particular bandwidth chosen (2–500 Hz for the Ca^{2+}-dependent current and 0.5–500 Hz for the M current).

Not all cells with Ca^{2+} transients showed the conductance changes. Among 45 cells expressing mAChR I or mAChR III, which were studied under patch-clamp conditions, 38 cells displayed a large Ca^{2+} transient. In 27 of these cells a clearcut outward current was observed and the conductance increase (slope conductance around −60 mV) ranged from 0.10 to 3.25 nS with a mean of 1.05 ± 0.14 nS. The conductance decrease was observed in 19 out of 30 cells expressing either mAChR I or mAChR III, ranging from 0.05 to 0.5 nS.

The conductance increase during Ca^{2+} transients was specific for K^+. This was shown by recordings at different external K^+ concentrations (5.5 mM and 20 mM), as exemplified in fig.4. The holding potential was jumped between three different levels and the reversal potential was estimated from current values at these different membrane potentials. In 20 mM K^+-saline it was −50 mV

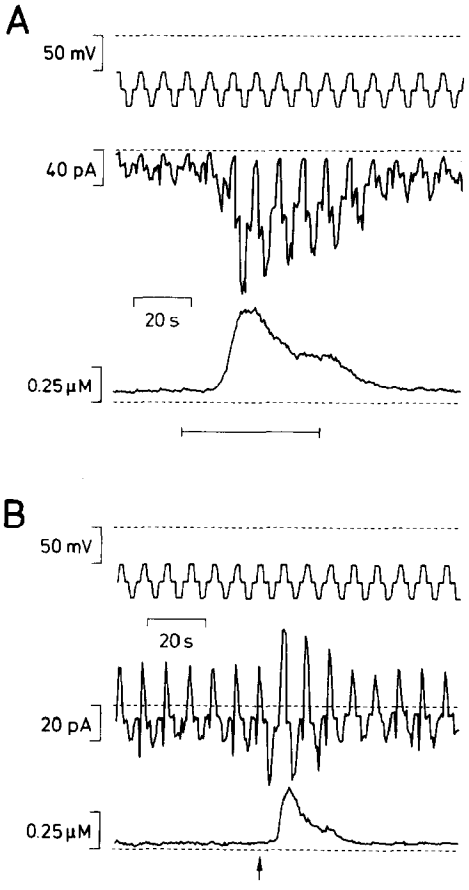

Fig.4. Reversal potential of Ca^{2+}-dependent currents. A porcine mAChR I-transformed cell (clone NGPM1-8) was clamped with a pipette containing standard internal filling solution. The potential was held at −75 mV and alternatingly clamped to −98 and −51 mV for periods of 2 s each. The uppermost traces in each panel represent the command potential, the center traces represent the membrane current, and the lowermost traces indicate changes in $[Ca^{2+}]_i$. The baselines are indicated by broken lines. (A) The cell was bathed in 20 mM K^+-saline. For the time indicated (bar) the chamber was perfused with the same solution supplemented with 5 μM ACh. (B) The same cell was bathed in standard external saline (5.5 mM K^+). It was stimulated by a puff of ACh-containing standard saline (5 μM ACh) applied from a closeby pipette (arrow). Note the difference in reversal potential, which is close to −51 mV in (A) and close to −75 mV in (B).

(fig.4A). The reversal potential measured in the same cell at normal (5.5 mM) external K^+ concentration was −72 mV (fig.4B). The mean reversal potential at 5.5 mM K^+ in 10 cells was −72 ± 2 mV, whereas that at 20 mM K^+ was −47 mV (2 experiments). This shift of reversal potential cor-

responds to the prediction of the Nernst equation for K^+ and shows that the channel has a permeability ratio for K^+ over Na^+ larger than 10.

In some recordings, internal Ca^{2+} was buffered by a high concentration of BAPTA (10 mM). Ca^{2+} transients and ACh-induced conductance increases were not observed under these conditions (5 experiments). This shows that the K^+ current elicited by ACh is Ca^{2+}-dependent.

In addition to the conductance changes described above, ACh application sometimes caused a burst of channel openings of large amplitudes. Inward single-channel currents of this type were well resolved in the whole-cell recording. They had an amplitude of 10–15 pA at −90 mV and of 5–8 pA at −40 mV. These channels were observed infrequently and were not studied in detail.

4. DISCUSSION

Our results demonstrate that two subtypes of the muscarinic acetylcholine receptor, mAChR I and mAChR III, are able to elicit Ca^{2+} release. Essentially no such response is observed with cells expressing mAChR II or mAChR IV. Responses in individual cells with mAChR I or mAChR III displayed many features of a regenerative process. Thus, the rising phase of the $[Ca^{2+}]_i$ increase was highly sigmoid starting after a characteristic delay, and the response was 'all-or-nothing' in the sense that at low ACh concentration there was a high percentage of cells that did not respond at all. Nevertheless the mean increment in $[Ca^{2+}]_i$ of responding cells was a graded function of ACh concentration. Both mAChR I-transformed and mAChR III-transformed cells showed these qualitative features. In both cases, the delay was linearly dependent on the reciprocal of ACh concentration. According to a kinetic model of phospholipase C activation and of Ca^{2+} release ([25] and Marty, A., Tan, Y., Horn, R. and Zimmerberg, J., in preparation) the delay of the response (d) follows the equation

$$d = (1 + K_D'/A)e/R_T \quad (1)$$

where K_D' is the apparent dissociation constant for ACh, A is the ACh concentration, e is a constant reflecting the efficacy of an activated receptor in eliciting Ca^{2+} release and R_T is the total number of receptors. Thus, the intercept of plots of the kind shown in fig.2 with the abscissa should give the value of K_D'. As shown in table 1, the K_D' values are close to 0.2 μM for both clones expressing mAChR III. The plots for the two clones expressing mAChR I give less reliable K_D' values (3.0 and 1.7 μM) as the regression lines come close to the origin. A more accurate estimate of the K_D' for mAChR I-transformed cells would require kinetic results with a time resolution better than was achieved in the present study. The K_D' for these clones is however unquestionably larger (by a factor close to 10) than the value of 0.2 μM obtained for the mAChR III-transformed clones. Thus, mAChR III has a higher affinity for agonist than mAChR I. In accord with this result, it has been shown that mAChR III, as compared with mAChR I, has a higher sensitivity to agonist in mediating activation of a Ca^{2+}-dependent Cl^- current in *Xenopus* oocytes and stimulation of PI hydrolysis in NG108-15 cells and that mAChR III has a higher binding affinity for agonist than mAChR I [11]. Another useful comparison can be made with the value (0.27 μM) obtained by the method illustrated in fig.2 for rat lacrimal gland cells [25]. The similarity to the K_D' value for mAChR III suggests that these cells preferentially express mAChR III. This is consistent with the results of the RNA blot hybridization analysis which show that porcine lacrimal gland contains both the mAChR I and mAChR III mRNAs [27] and that rat pancreas contains the mAChR III mRNA [13].

Concomitantly with the $[Ca^{2+}]_i$ rise, muscarinic stimulation elicited the opening of a Ca^{2+}-dependent K^+ channel. Noise analysis showed that this channel had a small unitary conductance (2.7 pS, uncorrected for open probability). These findings together with those of Fukuda et al. [9] indicate that the Ca^{2+}-dependent K^+ channel resembles the small-conductance, apamin-sensitive Ca^{2+}-dependent K^+ channel of hepatocytes [28]. The unitary conductance is appreciably smaller than the value (10–14 pS) reported for other apamin-sensitive Ca^{2+}-dependent K^+ channels present in skeletal muscle membranes [1]. However, the latter values were obtained at high-external K^+ concentration. A few data points at 5.6 mM external K^+ concentration given by Lang and Ritchie [29] for a Ca^{2+}-dependent K^+ channel in GH_3 cells

indicate a slope conductance of 4 pS at negative membrane potentials.

Comparison of noise levels before and after ACh application gave an estimate of the single-channel conductance for the M current of 3.15 pS. Spectral analysis indicated a mean channel open time or a mean duration of bursts in the range of 100 ms. The fact that the current decrease was not reversible after removal of ACh suggests that some diffusible intracellular factor is necessary for such a recovery and that this compound may be lost in whole-cell recording.

Acknowledgements: This work was supported in part by a grant of the Deutsche Forschungsgemeinschaft to E.N. (DFG-Ne 243-3) and by grants to S.N. from the Ministry of Education, Science and Culture of Japan, the Mitsubishi Foundation and the Japanese Foundation of Metabolism and Diseases.

REFERENCES

[1] Blatz, A.L. and Magleby, K.L. (1987) Trends Neurosci. 10, 463–467.
[2] Marty, A. (1987) Trends Neurosci. 10, 373–377.
[3] Fischmeister, R. and Hartzell, H.C. (1986) J. Physiol. 376, 183–202.
[4] Sakmann, B., Noma, A. and Trautwein, W. (1983) Nature 303, 250–253.
[5] Neer, E.J. and Clapham, D.E. (1988) Nature 333, 129–134.
[6] Brown, D. (1988) Trends Neurosci. 11, 294–299.
[7] Kubo, T., Fukuda, K., Mikami, A., Maeda, A., Takahashi, H., Mishina, M., Haga, T., Haga, K., Ichiyama, A., Kangawa, K., Kojima, M., Matsuo, H., Hirose, T. and Numa, S. (1986) Nature 323, 411–416.
[8] Fukuda, K., Kubo, T., Akiba, I., Maeda, A., Mishina, M. and Numa, S. (1987) Nature 327, 623–625.
[9] Fukuda, K., Higashida, H., Kubo, T., Maeda, A., Akiba, I., Bujo, H., Mishina, M. and Numa, S. (1988) Nature 335, 355–358.
[10] Akiba, I., Kubo, T., Maeda, A., Bujo, H., Nakai, J., Mishina, M. and Numa, S. (1988) FEBS Lett. 235, 257–261.
[11] Bujo, H., Nakai, J., Kubo, T., Fukuda, K., Akiba, I., Maeda, A., Mishina, M. and Numa, S. (1988) FEBS Lett. 240, 95–100.
[12] Peralta, E.G., Winslow, J.W., Peterson, G.L., Smith, D.H., Ashkenazi, A., Ramachandran, J., Schimerlik, M.I. and Capon, D.J. (1987) Science 236, 600–605.
[13] Peralta, E.G., Ashkenazi, A., Winslow, J.W., Smith, D.H., Ramachandran, J. and Capon, D.J. (1987) EMBO J. 6, 3923–3929.
[14] Ashkenazi, A., Winslow, J.W., Peralta, E.G., Peterson, G.L., Schimerlik, M.I., Capon, D.J. and Ramachandran, J. (1987) Science 238, 672–675.
[15] Peralta, E.G., Ashkenazi, A., Winslow, J.W., Ramachandran, J. and Capon, D.J. (1988) Nature 334, 434–437.
[16] Bonner, T.I., Buckley, N.J., Young, A.C. and Brann, M.R. (1987) Science 237, 527–532.
[17] Jones, S.V.P., Barker, J.L., Bonner, T.I., Buckley, N.J. and Brann, M.R. (1988) Proc. Natl. Acad. Sci. USA 85, 4056–4060.
[18] Lai, J., Mei, L., Roeske, W.R., Chung, F.-Z., Yamamura, H.I. and Venter, J.C. (1988) Life Sci. 42, 2489–2502.
[19] Nirenberg, M., Wilson, S., Higashida, H., Rotter, A., Krueger, K., Busis, N., Ray, R., Kenimer, J.G. and Adler, M. (1983) Science 222, 794–799.
[20] Hamprecht, B., Glaser, T., Reiser, G., Bayer, E. and Propst, E. (1985) Methods Enzymol. 109, 316–341.
[21] Marty, A. and Neher, E. (1983) in: Single-Channel Recording (Sakmann, B. and Neher, E. eds) pp.107–122, Plenum, New York.
[22] Grynkiewicz, G., Poenie, M. and Tsien, R.Y. (1985) J. Biol. Chem. 260, 3440–3450.
[23] Almers, W. and Neher, E. (1985) FEBS Lett. 192, 13–18.
[24] Neher, E. (1988) J. Physiol. 395, 193–214.
[25] Horn, R. and Marty, A. (1988) J. Gen. Physiol. 92, 145–159.
[26] Neher, E. and Stevens, C.F. (1977) Annu. Rev. Biophys. Bioeng. 6, 345–381.
[27] Maeda, A., Kubo, T., Mishina, M. and Numa, S. (1988) FEBS Lett. 239, 339–342.
[28] Capiod, T., Field, A.C., Ogden, D.C. and Sandford, C.A. (1987) FEBS Lett. 217, 247–252.
[29] Lang, D.G. and Ritchie, A.K. (1987) Pflügers Arch. 410, 614–622.